In-vivo reliability assessment of Intravoxel incoherent motion diffusion weighted MRI parameters

Moti Freiman[1], Jeannette M Perez-Rossello[1], Michael J Callahan[1], Mark Bittman[1], Stephan D Voss[1], Robert V Mulkern[1], and Simon K Warfield[1]
[1]*Radiology, Children's Hospital Boston/Harvard Medical School, Boston, MA, United States*

Introduction: Diffusion-weighted MRI (DW-MRI) is a non-invasive imaging technique sensitive to the thermally-driven, random motion of water molecules modified in living tissue by the interaction with cell membranes and macromolecules. The intra-voxel incoherent motion bi-exponential model (IVIM), as initially proposed by Le-Bihan et al. (1), attempts to separate this intra- and extracellular water diffusion from the incoherent motion of water molecules within randomly oriented capillaries. Several studies have utilized IVIM DW-MRI parameters for various clinical applications in the abdomen including the differential analysis of tumors and the assessment of liver cirrhosis. The presence of noise and patient motion in the acquired DW-MRI images, which cannot be eliminated completely through post-processing or special acquisition techniques, may substantially affect IVIM parameter estimation reliability. It is therefore critical to assess the *in-vivo* IVIM model parameters reliability in order to rely upon it for clinical evaluation.

Commonly used IVIM model fitting methods treat the model fitting as an optimization problem and provide only point estimate of the IVIM parameters without assessing the fit reliability (Fig. 1). The error propagation function used to relate error in the measured signal due to noise to estimated parameters proposed in (2) assumed that noise is independent and identically distributed (IID). This assumption does not hold for motion related artifacts which are not IID and therefore cannot reflect the actual fit reliability. Bayesian model fitting, proposed in (3), can provide both the IVIM model parameters estimates and assess the fit reliability through the estimation of the variance of each parameter. However, it requires numerical integration of the marginal posterior probabilities over the possible parameter value ranges, which is sensitive both to discretization/sampling effects and to the chosen integration limits (4). Direct estimation of the IVIM model parameter fits reliability through calculation of the confidence intervals (CI) can be accomplished using multiple point fits or repeated-sampling bootstrap (5) to construct the fit distribution. However, this is impracticable in routine clinical use due to lengthy scan times per patient, and to resulting increases in artifacts. Model-based bootstrap techniques for reliability assessment without requiring multiple acquisitions assumes underlying linear model. Hence, they cannot utilize directly for reliability assessment of the bi-exponential IVIM model. Recently, the unscented wild-bootstrap was proposed as a method to assess fit reliability for the bi-exponential IVIM model (6). In this work, we demonstrate the feasibility of *in-vivo* assessment of the achievable IVIM fit reliability in free-breathing body DW-MRI scans in a clinical setting with the unscented wild-bootstrap method (6).

Materials and Methods: We obtained images from 15 subjects; 9 males and 6 females with a mean age of 14.13 (range 7-24, std 4.09) that underwent MRI studies between Sep. 2010 and Mar. 2011. We carried out MR imaging studies of the abdominal organs using a 1.5-T unit (Magnetom Avanto, Siemens Medical Solutions, Erlangen, Germany) and a body-matrix coil and spine array coil for excitation and receiving. We performed free-breathing single-shot echo-planar imaging using the following parameters: repetition time/echo time (TR/TE) = 6800/59 ms, SPAIR fat suppression, matrix size = 192×156, field of view = 300×260 mm, number of excitations = 1, slice thickness/gap = 5 mm/0.5 mm, 40 axial slices, 8 b-values = 5,50,100,200,270,400,600,800 s/mm^2. A tetrahedral gradient scheme, first proposed by Conturo et al. (7), was used to acquire 4 repeated images at each b-value with a scan time of 4 min. Regions of Interest were drawn for the liver, kidneys and the spleen, both within the organ, and near the organs' boundaries. The IVIM model was fitted to the data for each voxel in the ROI, and the non-parametric unscented wild-bootstrap technique (6) was used to estimate the 95% CI of each of the IVIM parameters (i.e. D, D^*, f) at each voxel. Averaged IVIM values with their averaged 95% CI were calculated over these regions. Fit reliability was defined as the ratio between the 95% CI size and the averaged IVIM parameter value (i.e. smaller is better). Two-tailed student's t-test was used to assess the difference in the IVIM values and the fit reliability between the different regions of each organ.

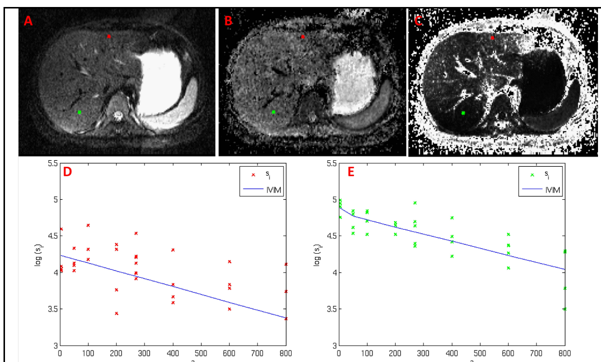

Fig. 1: Representative example of the fitted curves at boundary (red) and inner (green) voxels in the liver. (A) Anatomical image (b-value=5 s/mm^2), (B) D parametric map, (C) Fit reliability map computed using (6) (brighter means lower reliability), (D) measured signal and the fitted IVIM model for less reliable fit (red dot), and; (E) measured signal and the fitted IVIM model for more-reliable fit (green dot).

Results: Fig. 1 presents representative examples of the fitted IVIM curves to a boundary voxel and to an inner voxel, along with the anatomical image and the fit reliability map generated using (6). The observed signal is more affected by respiratory motion in the organ's boundary, which yielded a lower fit reliability as compared to the inner region of the organ. Table 1 depicts average IVIM model parameters values along with the fit-reliability measure for the different regions within each organ. While there was no significant difference in the D value between boundaries and the interiors of each organ, the fit reliability was significantly lower at or near organ boundaries. The fit reliability of the D parameter was substantially higher in the kidneys as compared to the liver and the spleen. This reflects their higher stability during respiratory motion. The overall fit reliability of the D^* and f parameters was much lower as compared to the overall fit reliability of the D parameter. Fit reliability was lower at the organs' boundaries as compared to the regions inside the organs for all organs and IVIM parameters.

Discussion: Fit reliability assessment in IVIM model fitting to DW-MRI data is an important aspect to consider if IVIM analysis is to be used in clinical decision making. Significant differences in fit reliability across different regions encourage careful selection of regions for IVIM analysis. We have demonstrated that IVIM fit reliability can be measured *in-vivo* from clinical DW-MRI data using the unscented wild-bootstrap. The computed fit reliability maps were able to separate the organs' boundaries where motion artifacts highly reduce the IVIM fit reliability from the interior regions which are more stable and so produce more reliable IVIM fits. The computed fit reliability maps can serve as an *in-vivo* quality control tests to evaluate the overall DW-MRI scan quality and its usefulness for reliable quantitative analysis. Moreover, these maps can guide the radiologist during the selection region of interest selection for reliable IVIM analysis.

Table 1		Liver			Kidney			Spleen		
		boundary	interior	p-value	boundary	interior	p-value	boundary	interior	p-value
D	Averaged value (μm^2/ms)	1.3	1.2	0.24	1.9	1.9	0.9	1.2	0.8	0.08
	Fit reliability	49.15	29.07	0.029*	21.85	11.6	0.005*	59.02	33.8	0.002*
D*	Averaged value (μm^2/ms)	18.9	21	0.13	18	15.9	0.31	20.5	17.5	0.032*
	Fit reliability	361.4	318.7	0.04*	325.9	277.2	0.15	371.1	342.4	0.15
f	Averaged value	0.16	0.13	0.17	0.2	0.08	0.006*	0.65	0.06	0.027*
	Fit reliability	259.1	222.1	0.07	385.75	232.4	0.07	773	282.4	$2*10^{-5}$*

Bibliography:

1. Le Bihan D, et al. Radiology 1988;168(2):497-505.
2. Zhang JL, et al. Magn Reson Med 2011, in press.
3. Neil JJ, Bretthorst GL. Magn Reson Med 1993;29(5):642-647.
4. Behrens TE, et al. Magn Reson Med 2003;50(5):1077-1088.
5. Efron B, Tibshirani RJ. An Introduction to the Bootstrap. New York: Chapman & Hall: 1993.
6. Freiman M, et al. Med Image Comput Comput Assist Interv 2011;14(Pt 2):74-81.
7. Conturo TE, et al. Magn Reson Med 1996;35(3):399-412.